Liver International

WILEY

Liver INTERNATIONAL

ORIGINAL ARTICLE OPEN ACCESS

Liver Metabolomic Profiling Reveals Distinct Signatures Between Steatosis and Metabolic Dysfunction-Associated Steatohepatitis

Saana Palomurto[1,2] | Emily Flam[3] | Dorota Kaminska[4,5,6] | Kirsi A. Virtanen[7] | Vesa Kärjä[8] | Pirjo Käkelä[1,2] | Päivi Pajukanta[4,9,10] | Delphine Eberlé[3] | Joel T. Haas[3] | Violeta Raverdy[3] | Robert Caiazzo[3] | François Pattou[3] | Bart Staels[3] | Jussi Pihlajamäki[5,11] | Ville Männistö[2,12]

[1]Department of Surgery, Kuopio University Hospital, North Savo Wellbeing County, Kuopio, Finland | [2]School of Medicine, Institute of Clinical Medicine, University of Eastern Finland, Kuopio, Finland | [3]University of Lille, Inserm, CHU Lille, Institut Pasteur Lille, Lille, France | [4]Department of Human Genetics, David Geffen School of Medicine at UCLA, Los Angeles, California, USA | [5]Institute of Public Health and Clinical Nutrition, School of Medicine, University of Eastern Finland, Kuopio, Finland | [6]Division of Digestive Diseases, David Geffen School of Medicine at UCLA, Los Angeles, California, USA | [7]Turku PET Centre, University of Turku and Turku University Hospital, Turku, Finland | [8]Department of Clinical Pathology, Kuopio University Hospital, North Savo Wellbeing County, Kuopio, Finland | [9]Bioinformatics Interdepartmental Program, UCLA, Los Angeles, California, USA | [10]Institute for Precision Health, David Geffen School of Medicine at UCLA, Los Angeles, California, USA | [11]Department of Medicine, Endocrinology, and Clinical Nutrition, Kuopio University Hospital, North Savo Wellbeing County, Kuopio, Finland | [12]Department of Medicine, Internal Medicine, Kuopio University Hospital, North Savo Wellbeing County, Kuopio, Finland

Correspondence: Saana Palomurto (palomurt@uef.fi)

Received: 18 November 2025 | **Revised:** 26 January 2026 | **Accepted:** 29 January 2026

Handling Editor: Dr. Luca Valenti

Keywords: lipid metabolism | metabolomics | RNA-seq | systems biology | uridine disphosphate galactose

ABSTRACT

Background and Aims: Metabolic dysfunction-associated steatotic liver disease (MASLD), the most common chronic liver disease worldwide, is closely linked to obesity and metabolic syndrome. The reason some patients with MASLD develop metabolic dysfunction-associated steatohepatitis (MASH) and which metabolic changes in the liver are linked to its progression are unclear.

Methods: A non-targeted metabolomics analysis was performed on liver samples from 106 Finnish patients with severe obesity (71 females, mean age ± SD: 48.6 ± 8.7 years, body mass index: 41.6 ± 5.2 kg/m^2) selected for laparoscopic gastric bypass surgery. Liver metabolomics and liver RNA sequencing data were used to study metabolic differences between those with steatosis and those with MASH. Validation was performed in a French cohort of 227 patients with obesity and MASLD.

Results: Overall, 45 metabolites differed between patients with steatosis and those with MASH. Novel MASH-associated metabolites included N-acetylneuraminate ($\beta = 0.276$), pentose acid ($\beta = -0.290$), UDP-galactose ($\beta = -0.413$), gamma/beta-tocopherol ($\beta = -0.317$), and guanidinosuccinate ($\beta = -0.289$) (all $p < 0.05$). In the validation cohort, 8 of 20 metabolites, including N-acetylneuraminate and plasmalogens 1-(1-enyl-palmitoyl)-2-arachidonoyl-GPE(P-16:0/20:4) and 1-(1-enyl-stearoyl)-2-arachidon

---

Abbreviations: ABOS, Biological Atlas of Severe Obesity; BMI, body mass index; FDR, false discovery rate; GPC, glycerophospatidylcholine; GPE, glycerophosphatidylethanolamine; KEGG, Kyoto Encyclopedia of Genes and Genomes; KOBS, Kuopio Obesity Surgery Study; LC–MS/MS, liquid chromatography–tandem mass spectrometry; LRYGB, laparoscopic Roux-en-Y gastric bypass; MASH, metabolic dysfunction-associated steatohepatitis; MASLD, metabolic dysfunction-associated steatotic liver disease; MBOAT7, membrane-bound O-acyltransferase domain-containing 7; PCA, primary component analysis; PNPLA3, patatin-like phospholipase domain-containing 3; PPAR, peroxisome proliferator-activated receptor; SAF, steatosis activity and fibrosis; TG, triglycerides; TM6SF2, transmembrane 6 superfamily member 2; UDP, uridine disphosphate; VLCD, very-low-calorie diet.

Liver International, 2026; 46:e70552
https://doi.org/10.1111/liv.70552

oyl-GPE(P-18:0/20:4), were linked to MASH ($p < 0.05$). The 45 significantly altered metabolites formed two clusters with different associations with metabolic parameters, depending on their correlation with liver histological features. Kyoto Encyclopedia of Genes and Genomes analysis revealed that elevated metabolites in MASH were associated with inflammatory pathways; those decreased in MASH were linked to fatty acid degradation and amino acid and pyruvate metabolism.

Conclusion: Transitioning from simple steatosis to MASH is associated with distinct alterations in liver metabolites and systemic metabolic traits, highlighting disease progression-associated pathways.

1 | Introduction

The global prevalence of metabolic dysfunction-associated steatotic liver disease (MASLD), previously known as nonalcoholic fatty liver disease, is > 30% [1, 2]. The disease presents primarily as hepatic steatosis but can progress to metabolic dysfunction-associated steatohepatitis (MASH), fibrosis, cirrhosis and hepatocellular carcinoma [3–5]. The reason that steatosis progresses to MASH in approximately 16% of patients is unknown [6]. Lipidomic analyses of the liver tissue have demonstrated alterations in fatty acids in patients with MASH compared to those in patients with steatosis [7, 8]. MASH has also been associated with increased hepatic levels of aromatic and branched-chain amino acids [9]. However, comprehensive information regarding the pathogenesis of MASH and changes in liver metabolism in patients with MASH remains scarce.

Non-targeted metabolite profiling provides an intriguing opportunity to obtain a comprehensive picture of metabolic processes and pathophysiological alterations associated with the pathogenesis of MASH [10]. More specifically, focusing on liver tissue can provide an extensive view of the pathophysiological alterations in MASH, compared with measuring plasma or serum samples, which integrate the extrahepatic components of these processes [11].

In this study, we investigated the alterations in liver metabolites in individuals with severe obesity and with and without MASLD using non-targeted relative quantitative liquid chromatography–tandem mass spectrometry (LC–MS/MS), focusing on the differences between steatosis and MASH. Our main findings were validated using an external cohort study. Furthermore, the associations between the most significantly altered metabolites and metabolic disturbances were analysed. Finally, liver RNA sequencing data were used to identify the metabolic pathways responsible for the observed changes.

2 | Methods

2.1 | Kuopio Obesity Surgery (KOBS) Cohort

Overall, 106 individuals who underwent laparoscopic Roux-en-Y gastric bypass (LRYGB) for the treatment of severe obesity were selected from the KOBS study [12] based on the availability of liver tissue for metabolomic analysis, fasting serum samples, and detailed liver histological characterisations.

Clinical features, medical history and medication use were recorded during an outpatient visit before surgery. All patients were instructed to follow a very-low-calorie diet (VLCD) for approximately 4 weeks before surgery, and blood samples were collected after 12 h of fasting the morning before the operation. Plasma glucose, insulin and serum lipid levels were measured, as previously described [13]. Patatin-like phospholipase domain-containing 3 (*PNPLA3*) I148M at rs738409, transmembrane 6 superfamily member 2 (*TM6SF2*) rs58542926 C > T, and membrane-bound O-acyltransferase domain-containing 7 (*MBOAT7*) rs641738 C > T were genotyped using the TaqMan SNP genotyping assay (Applied Biosystems), according to the manufacturer's protocol. The study was conducted in accordance with the principles of the Declaration of Helsinki and Istanbul. Written informed consent was obtained from all participants before the study procedure. The study protocol was approved by the Ethics Committee of Northern Savo Hospital District (54/2005, 104/2008, 27/2010 and 1108/2018).

2.2 | Validation Cohort

To validate our metabolite analysis, we utilised an independent external cohort ($n = 227$) from the Biological Atlas of Severe Obesity (ABOS) cohort [14], which included liver biopsies and plasma from patients with steatosis ($n = 146$) or MASH ($n = 81$). The clinical characteristics of the validation (ABOS) cohort are presented in Table S1. Liver and plasma metabolomic profiling in this cohort was performed using the same Metabolon platform and methodology as for the KOBS cohort, as described later in the text [14]. A linear regression model, adjusted for age and sex, was applied to the 25 top-ranked metabolites identified in the KOBS cohort in our primary analysis to replicate their association with steatosis and MASH.

2.3 | Liver Histology

Wedge biopsies of the liver tissue were collected during elective LRYGB. The samples in the KOBS cohort were graded using the Steatosis, Activity and Fibrosis (SAF) scoring system [15], whereas the samples in the ABOS cohort were graded according to the NASH Clinical Research Network scoring system [16]. For analytical comparability, patients with definite steatohepatitis (NASH CRN) or MASH (SAF ≥ S1A2) were categorised together as having steatohepatitis, and fibrosis stages were analysed on a unified 0–4 scale, which is identical in both systems.

2.4 | Non-Targeted Metabolomics

2.4.1 | Metabolomics Analysis

Non-targeted metabolomic profiling of plasma and fresh frozen liver samples was performed by Metabolon Inc. (Durham, NC, USA). Briefly, methanol extraction of biochemicals was

Key Points

- Using non-targeted liver metabolomics, we identified distinct metabolic alterations that differentiate simple steatosis from MASH in patients with severe obesity.
- Several novel metabolites, including N-acetylneuraminate, UDP-galactose, pentose acid and specific plasmalogens, were associated with MASH and showed partial replication in an external cohort in the liver.
- MASH-associated metabolites clustered into biologically distinct patterns linked to systemic metabolic traits and liver histological features.
- Integrated metabolomic and transcriptomic pathway analyses revealed that these metabolite clusters were linked to distinct biological processes, with metabolites elevated in MASH associated with inflammatory pathways and those reduced in MASH linked to fatty acid, amino acid and pyruvate metabolism.

followed by non-targeted relative quantitative LC–MS/MS. The Metabolon DiscoveryHD4 platform was used to assay the metabolites.

All samples were processed for peak quantification and scaling. Raw mass spectrometry peaks were quantified for each metabolite using the area under the curve, and the overall process variability was evaluated using the median relative SD for endogenous metabolites present in all 20 technical replicates in each batch. Samples were adjusted for variations caused by day-to-day instrument tuning differences and columns used for biochemical extraction by scaling the raw peak quantifications to the median for each metabolite in the Metabolon batch.

2.4.2 | Data Analysis

After data preprocessing, which included natural logarithm conversion, a *t*-test and linear model adjusted for age and sex were used to identify metabolites that differed significantly between patients with steatosis and those with MASH. The same analysis was performed on the validation cohort after identical preprocessing.

For the discovery cohort, primary component analysis (PCA) was used to identify the differences between liver phenotypes (normal liver, steatosis and MASH). A *t*-test was performed to further assess which metabolites differed between those with a normal liver, steatosis or MASH. Spearman's correlation with *K*-means clustering was used to analyse the associations between metabolites and measurements reflecting metabolic disturbances. The metabolites for the correlation analysis were chosen based on the linear regression analysis results. Statistical significance was set at $p < 0.05$. Our cross-sectional study had a large number of annotated metabolites ($n = 872$) relative to the sample size ($n = 106$). To provide a broad overview of metabolic alterations in MASH pathogenesis, we selected metabolites for further analysis based on unadjusted *p*-values. All statistical analyses and visualisations were performed using R (version 4.4.1; The R Project for Statistical Computing).

2.4.3 | RNA Sequencing

Total RNA sequencing was performed on liver samples from the KOBS study cohort, as previously described [17]. Libraries were subjected to paired-end sequencing (50-nucleotide reads) and subsequent read alignment. Gene-level counts were normalised using the trimmed mean of *M*-values method, converted to counts per million using edgeR, and subjected to $\log_2$ transformations. Expression data were corrected for technical covariates (RNA integrity number, percentage of uniquely aligned reads, and 3′ bias). To assess the association between gene expression and metabolite levels, partial Spearman correlation analysis, controlling for age, body mass index (BMI) and sex, was conducted on a subset of 34 samples with available metabolite and RNA-seq data.

2.4.4 | Pathway Enrichment Analysis

Enrichment analysis was conducted using the clusterProfiler R package, with genes annotated to the Kyoto Encyclopedia of Genes and Genomes (KEGG) pathways retrieved from the org.Hs.eg.db database. Pathways with an adjusted *p*-value (false discovery rate [FDR]) < 0.05 were considered significantly enriched. The enrichplot R package was used for data visualisation, and significant pathways were further explored to identify biological themes relevant to metabolic dysfunction. To integrate, visualise, and quantify the relationships between metabolites and KEGG pathways, a combined score was developed [18, 19]. This score incorporated two metrics: (1) the fold enrichment of genes in the pathway (retrieved during KEGG enrichment analysis) and (2) the correlation coefficients between gene expression and metabolite levels (derived from partial Spearman correlation analysis). These values were normalised to ensure comparability, and their product was used as the combined score. This score reflected the strength and direction of the metabolite-pathway association, integrating the gene-level contributions from both perspectives.

3 | Results

3.1 | Clinical Characteristics of the Study Populations

The KOBS cohort included 106 patients with severe obesity (71 females) with a mean ± SD age of 48.6 ± 8.7 years and a BMI of $41.6 \pm 5.2\,\text{kg/m}^2$. The demographic and clinical characteristics of the study cohort are presented in Table 1. Plasma ALT ($p < 0.001$), triglyceride (TG) ($p = 0.031$), glucose ($p = 0.002$) and insulin ($p = 0.002$) concentrations were higher in patients with MASH than in those with normal livers or steatosis. LDL cholesterol levels differed between the groups ($p = 0.042$), and patients with MASH showed lower LDL cholesterol levels than those with steatosis. In addition, the presence of type 2 diabetes ($p < 0.001$) and the use of cholesterol-lowering medications ($p = 0.010$) differed between the groups.

TABLE 1 | Clinical characteristics of the KOBS cohort.

	Total $n = 106$	Normal liver $n = 37$	Steatosis $n = 40$	MASH $n = 29$	p
Sex, female n (%)	71 (67.0)	29 (78.4)	24 (60.0)	18 (62.1)	0.185
Age (years)	48.6 ± 8.7	48.5 ± 8.6	48.3 ± 10.0	49.3 ± 7.1	0.913
BMI (kg/m^2)	41.6 ± 5.2	41.6 ± 5.4	40.5 ± 4.8	42.7 ± 5.4	0.335
Fasting glucose (mmol/L)	6.4 ± 1.6	5.7 ± 0.7	6.5 ± 1.4	7.1 ± 2.3	**0.002**
Fasting insulin (mIU/L)	18.3 ± 10.3	13.3 ± 7.3	18.8 ± 7.7	23.0 ± 13.3	**0.002**
ALT (U/L)	42.3 ± 28.1	28.4 ± 13.0	47.1 ± 35.0	52.8 ± 25.8	**< 0.001**
Total cholesterol (mmol/L)	4.2 ± 1.0	4.5 ± 0.9	4.2 ± 1.1	3.9 ± 0.9	0.077
LDL-cholesterol (mmol/L)	2.4 ± 0.9	2.7 ± 0.9	2.4 ± 1.0	2.1 ± 0.6	**0.042**
HDL-cholesterol (mmol/L)	1.2 ± 0.3	1.3 ± 0.3	1.2 ± 0.3	1.1 ± 0.3	0.206
Triglycerides (mmol/L)	1.5 ± 0.5	1.3 ± 0.5	1.5 ± 0.4	1.7 ± 0.6	**0.031**
Diabetes n (%)	37 (34.9)	1 (2.7)	16 (40.0)	20 (69.0)	**< 0.001**
Cholesterol medication n (%)	22 (20.8)	4 (10.8)	7 (17.5)	11 (37.9)	**0.010**

Note: The chi-square test was used to compare categorical variables, and the Kruskal-Wallis test was used for continuous variables. Results are presented as mean±SD. A p-value < 0.05 was considered significant and marked with a bold font.
Abbreviations: BMI, body mass index; MASH, metabolic dysfunction-associated steatohepatitis.

The validation (ABOS) cohort included 227 patients (145 females) with a mean age of 43.6 ± 10.9 years and a BMI of 46.8 ± 8.1 kg/m^2. The clinical characteristics of the validation cohort are presented in Table S1.

3.2 | Several Liver Metabolites Differed Between Steatosis and MASH

The metabolite PCA performed in the KOBS cohort did not reveal any significant differences in the distribution between patients with steatosis and those with MASH (Figure S1). Student's t-tests were conducted to assess how the metabolites differed among all histological groups (normal liver, steatosis and MASH) (Table S2). Overall, 112 metabolites differed ($p < 0.05$) between those with normal livers and those with steatosis, and 157 metabolites differed between those with normal livers and those with MASH. Furthermore, 45 metabolites differed between the patients with steatosis and those with MASH ($p < 0.05$; t-test and linear model adjusted for age and sex). These metabolites included 12 glycerophosphatidylcholines (GPC), 6 glycerophosphatidylethanolamines (GPE), 1 carnitine, 1 tocopherol, 1 ceramide and 24 other molecules (Table S3). The 25 most significant metabolites are shown in Figure 1, and all 45 metabolites are presented in Figure S2. When adjusted for age, sex and BMI, 18 of the top 25 metabolites differed significantly (Figure S3 and Table S4). When adjusted for age, sex, and the presence of the *PNPLA3*, *MBOAT7* and *TM6SF2* risk variants, 11 of the top 25 metabolites differed significantly (Figure S4). In a model adjusted with age, sex, and usage of cholesterol-lowering medication, all the top 25 metabolites remained significant (Figure S5). When adjusting for age, sex and type 2 diabetes status, 21 of the top 25 metabolites remained significant (Figure S6).

3.3 | Validation in External Cohort Demonstrated Similar Metabolic Alterations Linked to MASH

Next, we validated the top 25 metabolites from the KOBS cohort in a French ABOS cohort by constructing a linear model adjusted for age and sex between the patients with steatosis and those with MASH. Of the original 25 metabolites, 8 differed significantly between patients with steatosis and those with MASH, and 5 metabolites were not detected in the validation cohort. The levels of 1-(1-enyl-palmitoyl)-2-arachidonoyl-GPE(P-16:0/20:4), 1-(1-enyl-stearoyl)-2-arachidonoyl-GPE(P-18:0/20:4), 1,2-dipalmitoyl-GPC(16:0/16:0), 1-palmityl-2-oleoyl-GPS(16:0/18:1), and N-acetylneuraminate were significantly higher in patients with MASH than in those with steatosis in both cohorts (Figure 1, Tables S3 and S5). The levels of 1-linoleoyl-2-arachidonoyl-GPC(18:2/20:4), 1,2-dilinoleoyl-GPC(18:2/18:2) and 1-linoleoyl-2-linolenoyl-GPC(18:2/18:3) were significantly lower in patients with MASH than in those with steatosis in both cohorts (Figure 1, Tables S3 and S5). N-acetylneuraminate and 1-linoleoyl-2-arachidonoyl-GPC(18:2/20:4) were strongly associated with MASH (FDR < 0.05; Table S5) in the ABOS cohort.

3.4 | Plasma Metabolomics

Plasma metabolomics was available from the ABOS cohort for the external validation cohort. Of the 25 liver-associated metabolites identified in the primary analysis, four were detectable in plasma (creatine, N-acetylneuraminate, $\beta-/\gamma$-tocopherol and guanidinosuccinate). Among these, only N-acetylneuraminate differed significantly between steatosis and MASH in plasma, showing the same direction of association as observed in liver tissue (Table S6). The remaining

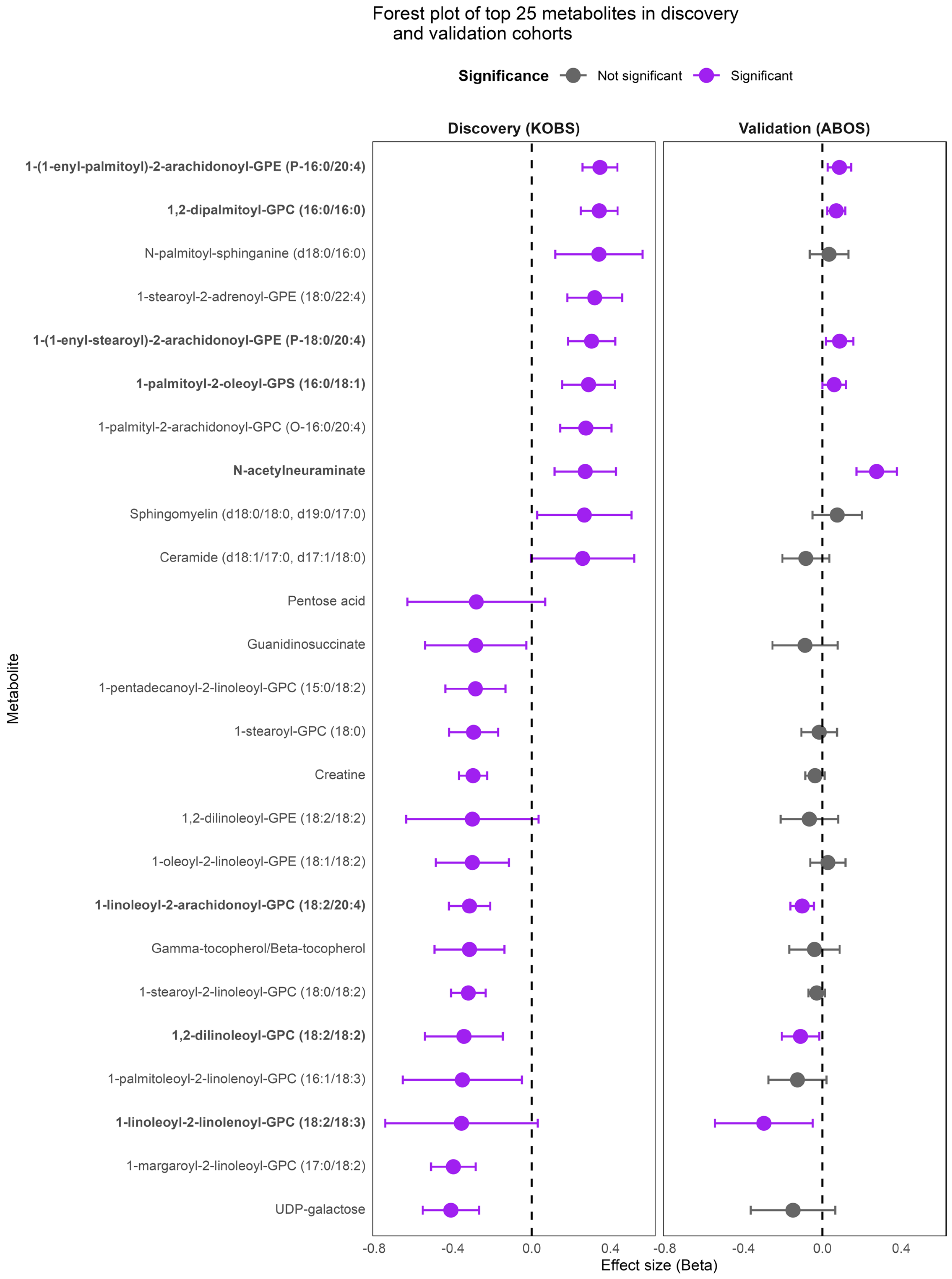

FIGURE 1 | Legend on next page.

FIGURE 1 | Forest plot representing the top 25 metabolites that differed significantly between patients with steatosis and those with MASH in a linear model adjusted for age and sex in the KOBS cohort ($n = 69$; left) and the ABOS validation cohort ($n = 227$; right). Significant metabolites in both cohorts are presented in bold. The lines around the dots represent 95% confidence intervals. $p < 0.05$ was considered significant. ABOS, Biological Atlas of Severe Obesity; GPC, glycerophosphatidylcholine; GPE, glycerophosphatidylethanolamine; GPS, glycerophosphatidylserine; KOBS, Kuopio Obesity Surgery Study; MASH, metabolic dysfunction-associated steatohepatitis; UDP-galactose, uridine diphosphate galactose.

metabolites did not show statistically significant differences in plasma.

3.5 | MASH-Associated Metabolites Have Two Distinct Metabolic Profiles

Next, we performed Spearman's correlation analysis in the KOBS cohort between the most significant metabolites and measurements reflecting metabolic disturbances, such as changes in insulin, glucose, lipid (total, LDL and HDL cholesterol and TG) levels and the BMI and liver histological parameters, which indicated conditions such as steatosis, lobular inflammation, ballooning and fibrosis. *K*-means clustering analysis of the correlation matrix identified two distinct clusters. The first cluster contained all 10 metabolites that were higher in patients with MASH than in those with steatosis, whereas the second cluster contained 15 metabolites that were lower in patients with MASH than in those with steatosis. The results of the correlation analysis for the top 25 metabolites are presented in Figure 2, and those for all significant metabolites are presented in Figure S7.

The metabolites in the first cluster were positively correlated with liver steatosis, lobular inflammation, ballooning, fibrosis, BMI and glucose, insulin, and TG levels and were negatively correlated with total, LDL and HDL cholesterol levels (Figure 2). This group included 6 phospholipids, 1 sphinganine, 1 sphingomyelin, 1 ceramide and N-acetylneuramite. The second cluster was negatively correlated with liver histology and glucose, insulin, and TG levels and was positively correlated with total, LDL and HDL cholesterol levels (Figure 2). It contained 15 metabolites, including γ-tocopherol/β-tocopherol, creatine, pentose acid, guanidinosuccinate, uridine diphosphate galactose (UDP-galactose) and 10 phospholipids, all of which, except for 1-stearoyl-GPC (18:0), contained linoleic or α-linolenic acid (Figure 2).

3.6 | MASH-Linked Metabolites Associate With Inflammatory Pathways

To study how metabolite levels are linked to liver gene expression, a partial Spearman correlation analysis, controlled for age, sex and BMI, was performed in the KOBS cohort of 34 patients with available overlapping data. UDP-galactose was negatively correlated with *MKI67* (FDR = 0.046), a gene encoding Ki-67, a protein required for cell proliferation. Guanidinosuccinate was positively correlated with *CYP4F3* (FRD = 0.046), whereas N-acetylneuraminate was negatively correlated (FDR = 0.032). *CYP4F3* encodes a cytochrome P450, which is involved in fatty acid metabolism. Guanidinosuccinate was correlated with the expression of 82 genes, including negative correlations with *GK* (FDR = 0.032), *ORMDL1* (FDR = 0.036) and *CPT1A* (FDR = 0.043), which regulate lipid and glucose metabolism. All gene expression-metabolite interactions with FDR < 0.1 are presented in Table S7.

To further explore the biological relevance of the 25 most significant MASH-associated metabolites, we conducted a KEGG pathway enrichment analysis based on genes significantly correlated with these metabolites. The analysis revealed significant enrichment of six pathways involved in T-cell receptor signalling (KEGG ID: hsa05340, FDR = 0.006), primary immunodeficiency (KEGG ID: hsa05340, FDR = 0.006), fatty acid degradation (KEGG ID: hsa00071, FDR = 0.006), 2-oxocarboxylic acid metabolism (KEGG ID: hsa01210, FDR = 0.006), pyruvate metabolism (KEGG ID: hsa00620, FDR = 0.008) and valine, leucine, and isoleucine degradation (KEGG ID: hsa00280, FDR = 0.008) (Figure 3a, Table S7).

A combined score (Section 2) was utilised to further demonstrate the relationship between metabolites and KEGG pathways, integrating pathway enrichment metrics with gene-metabolite correlations. This approach allowed us to identify biologically relevant pathways and provide insights into the potential mechanisms linking metabolite alterations to MASH in the KOBS cohort. Metabolites in cluster 1, including the plasmalogens 1-(1-enyl-palmitoyl)-2-arachidonoyl-GPE(P-16:0/20:4), 1-(1-enyl-stearoyl)-2-arachidonoyl-GPE(P-18:0/20:4) and 1-palmityl-2-arachidonoyl-GPC(O-16:0/20:4) as well as 1-palmitoyl-2-oleoyl-GPS(16:0/18:1), 1,2-dipalmitoyl-GPC(16:0/16:0), and N-acetylneuraminate were strongly associated with immune-related pathways, including primary immunodeficiency and T-cell receptor pathways (Figure 3b). In contrast, the 15 metabolites in cluster 2, which correlated negatively with liver histology, were enriched in metabolic pathways such as valine, leucine, and isoleucine degradation; pyruvate metabolism; fatty acid degradation; and 2-oxocarboxylic acid metabolism pathways (Figure 3b).

4 | Discussion

We performed a non-targeted metabolomic analysis of liver samples from individuals with severe obesity to identify the metabolites that differed between patients with steatosis and those with MASH. Analysis of 45 metabolites from metabolic pathways that differed between the groups revealed the novel association of N-acetylneuraminate, several lipids, pentose acid, guanidinosuccinate, UDP-galactose, and γ- and β-tocopherol with MASH. We validated eight of these metabolites (5 of 25 were not available) in the external ABOS cohort (Figure 1). In total, 19 of the 20 most significant metabolites showed a similar trend in relation to MASH in both cohorts. Only N-acetylneuraminate was significantly different based on the liver phenotype in plasma samples in ABOS (only four of

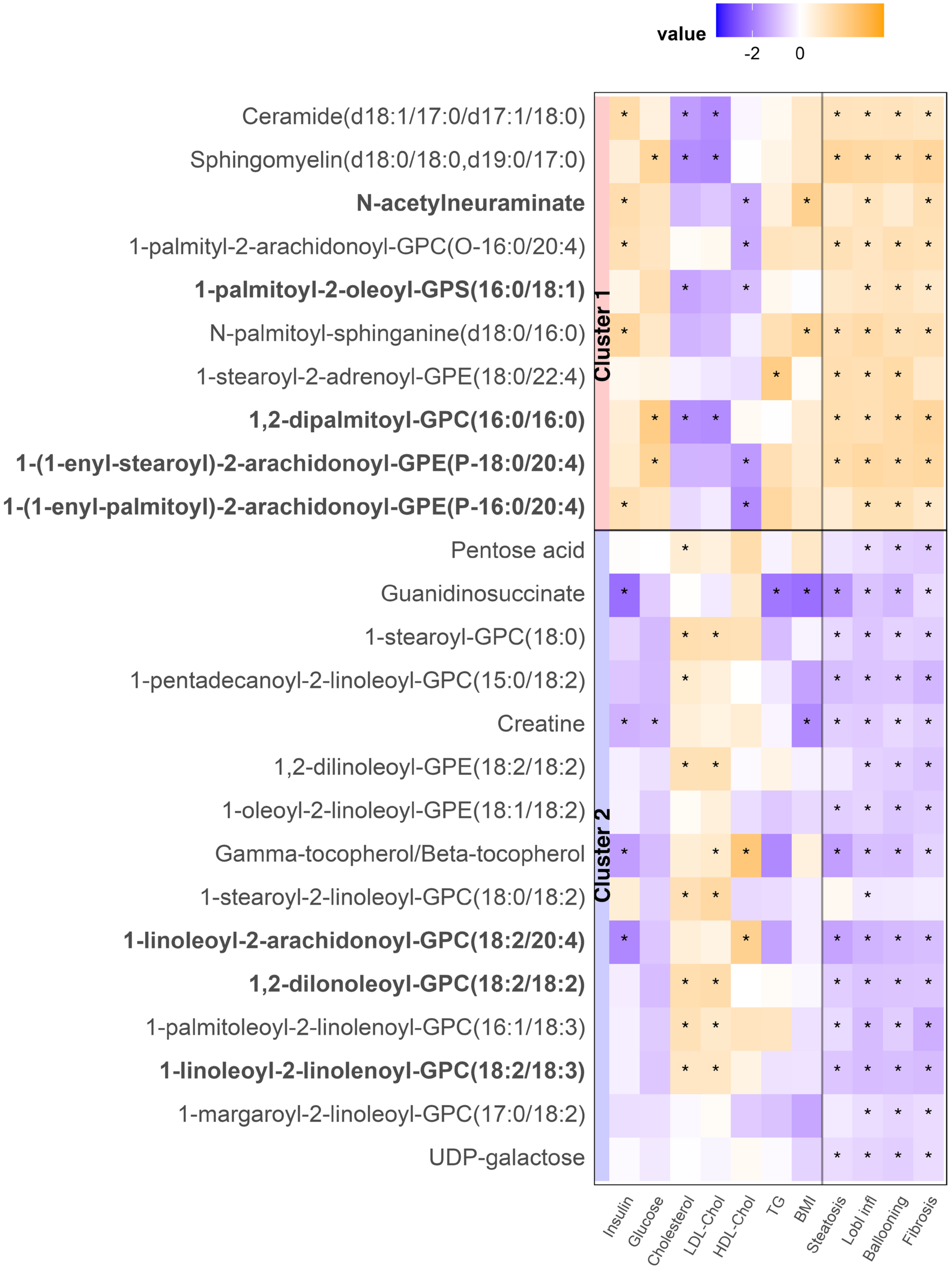

FIGURE 2 | Legend on next page.

FIGURE 2 | Heatmap representing associations (Spearman's correlation adjusted for age and sex) between 25 metabolites differing significantly between patients with steatosis and those with MASH (*y*-axis) and insulin, glucose, cholesterol, LDL cholesterol, HDL cholesterol and TG levels; BMI (*x*-axis, left side); and liver histology (horizontal row, right side). Metabolites that were significant in the validation (ABOS) cohort are bolded. *K*-means clustering was used to cluster metabolites based on their metabolic and histologic associations. The clusters are presented using red (cluster 1) and blue (cluster 2) bars. $*p < 0.05$. Positive correlations are presented in orange and negative correlations in purple. GPC; glycerophosphatidylcholine, GPE; glycerophosphatidylethanolamine, GPS; glycerophosphatidylserine, HDL-Chol; high-density lipoprotein cholesterol, LDL-Chol; low-density lipoprotein cholesterol, MASH; metabolic dysfunction-associated steatohepatitis, TG; triglyceride, UDP-galactose; uridine diphosphate galactose.

---

25 most significant liver metabolites were detected in plasma). The most significant 25 metabolites from the KOBS cohort were classified into two separate clusters that had divergent associations with measurements reflecting glucose and lipid metabolism, both of which are closely associated with MASH [20]. The metabolites that were lower in patients with MASH than in those with steatosis were negatively correlated with insulin, glucose and TG levels as well as the BMI and were positively correlated with total LDL- and HDL-cholesterol levels (cluster 2). In contrast, the metabolites that were higher in patients with MASH than in those with steatosis had the opposite correlation profile (cluster 1). These findings highlight a strong link between hepatic metabolic remodelling and systemic metabolic dysfunction in obesity-associated MASH.

A novel finding of this study was that N-acetylneuraminate, the predominant form of sialic acid in humans, was elevated in patients with MASH compared to those with steatosis in both the KOBS and ABOS cohorts, and it correlated positively with the BMI and insulin levels. Elevated serum sialic acid levels have been linked to insulin resistance in individuals with obesity [21] and observed in normal-weight/lean patients with MASLD [22]. In this study, the association between hepatic N-acetylneuraminate and MASH presence was attenuated after adjustment for type 2 diabetes status, suggesting that this metabolite may reflect more metabolic alterations closely linked to insulin resistance rather than MASH per se. However, N-acetylneuraminate was the only liver-associated metabolite that was significantly different in plasma between steatosis and MASH in the ABOS cohort.

The liver produces sialylated acute phase proteins in response to inflammation [23], and N-acetylneuraminate is an antioxidant [24]. N-acetylneuraminate was positively associated with T-cell receptor signalling and primary immunodeficiency pathways and positively correlated with lobular inflammation and fibrosis. Our finding of increased N-acetylneuraminate levels in patients with MASH may suggest that elevated hepatic N-acetylneuraminate reflects a state of hepatic oxidative stress and immune activation in MASH. Whether these associations extend to lean MASH or reflect obesity-specific mechanisms requires further investigation.

UDP-galactose was decreased in patients with MASH compared with those with simple steatosis. However, it did not reach statistical significance in the validation cohort. Both N-acetylneuraminate and UDP-galactose are key components of the protein glycosylation pathways, particularly in the synthesis and terminal modification of N-glycans [25, 26]. Glycosylation reactions are the most common posttranslational modifications of proteins and are often affected by cancer and other diseases, including liver inflammation, MASH, and fibrosis [27, 28]. N-glycan modifications and other products of the glycosylation process have been extensively studied to identify clinical biomarkers that could differentiate steatosis from MASH [28, 29]. Our findings may reflect the underlying dysregulation of hepatic glycosylation pathways in MASH, supporting the hypothesis that altered N-glycan biosynthesis and modification contribute to disease progression [27–29].

Interestingly, UDP-galactose did not correlate with the serum markers of glucose and lipid metabolism and remained significant when the linear model was adjusted for the BMI. This suggests that UDP-galactose is associated with MASH, independent of the metabolic disturbances typically associated with the disease. UDP-galactose and UDP-glucose are ligands for P2Y14 receptors in hepatic stellate cells, linking UDP-galactose to liver fibrogenesis [30]. Indeed, UDP-galactose negatively correlated with *MKI67*, which encodes the proliferation marker Ki-67, suggesting a potential link between decreased UDP-galactose levels and increased cellular proliferation. Ki-67 is expressed during all active cell-cycle phases and is a histological marker of cancer cell proliferation [31].

Levels of the plasmalogens 1-(1-enyl-palmitoyl)-2-arachidonoyl-GPE(P-16:0/20:4), 1-(1-enyl-stearoyl)-2-arachidonoyl-GPE(P-18:0/20:4), 1,2-dipalmitoyl-GPC(16:0/16:0) and 1-palmityl-2-oleoyl-GPS(16:0/18:1) were significantly higher in patients with MASH than in those with steatosis in both cohorts. Plasmalogens have been proposed to act as endogenous antioxidants [32, 33], and plasmalogen levels in serum lipoproteins decrease during oxidation [34]. Our results regarding the plasmalogens 1-(1-enyl-palmitoyl)-2-arachidonoyl-GPE(P-16:0/20:4) and 1-(1-enyl-stearoyl)-2-arachidonoyl-GPE(P-18:0/20:4) suggest that the liver upregulates plasmalogen synthesis in peroxisomes during oxidative stress. Increased levels of hepatic palmitic acid have been reported in patients with MASH compared to those in patients with steatosis [7], and our results are in line with this finding. In both cohorts, the levels of 1-linoleoyl-2-arachidonoyl-GPC(18:2/20:4), 1,2-dilinoleoyl-GPC(18:2/18:2) and 1-linoleoyl-2-linolenoyl-GPC(18:2/18:3) were significantly lower in patients with MASH than in those with steatosis. Interestingly, lipidomic profiling of HDL phospholipids has shown that GPCs with increased amounts of palmitic, palmitoleic or oleic acids and decreased amounts of linoleic acid are associated with metabolic syndrome [35]. Our results suggested a similar profile of liver phospholipids in patients with MASH.

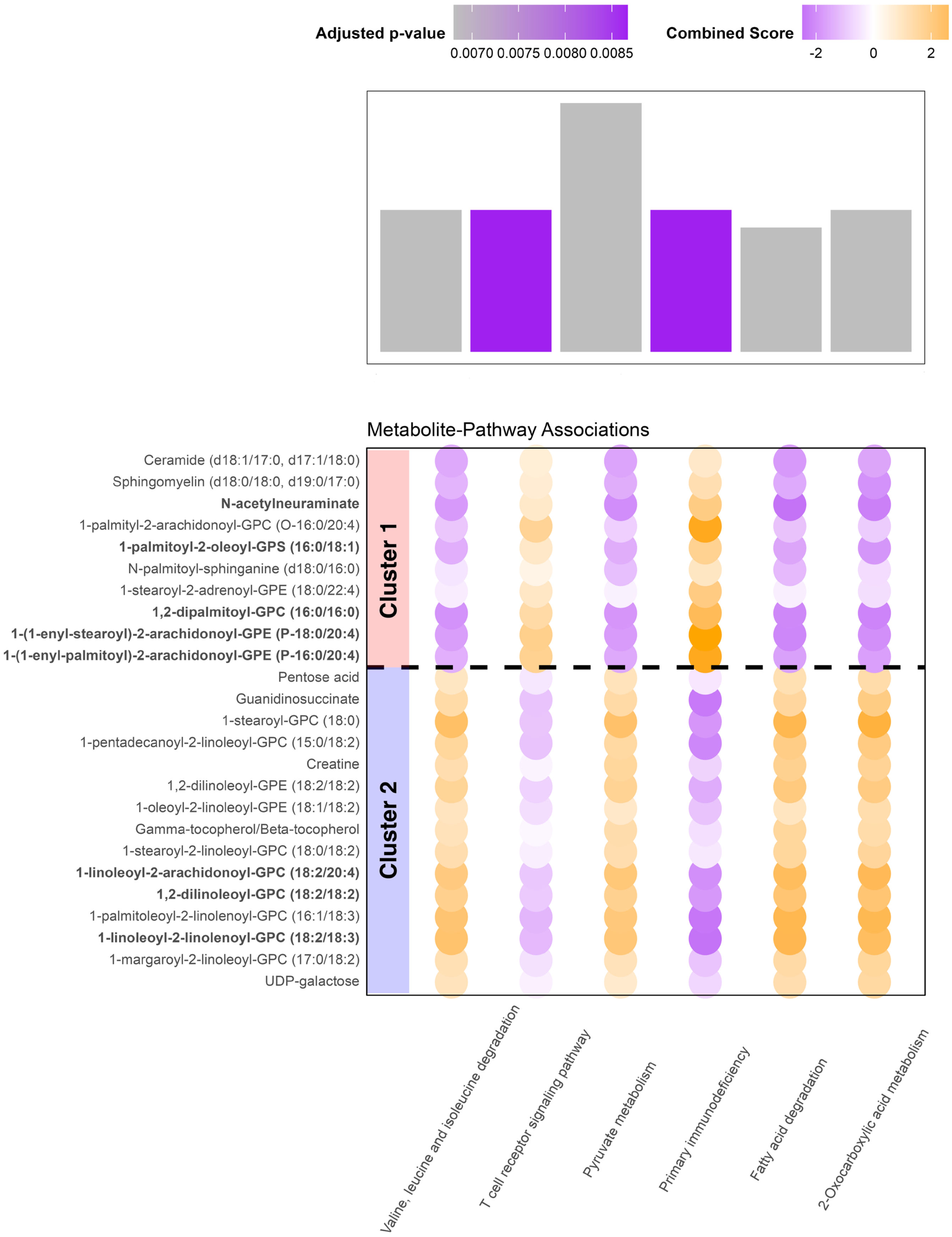

FIGURE 3 | Legend on next page.

FIGURE 3 | Bar plot of KEGG pathway enrichment analysis results based on genes associated with the top 25 metabolites that differed between simple steatosis and MASH in a linear model. The most significant pathways are displayed on the *x*-axis, and gene counts associated with each pathway are on the *y*-axis. The bar colour represents the adjusted *p*-value (FDR) of associations between the gene and pathway. Below the barplot is a dot plot representing associations between the pathways (*x*-axis) and metabolites (*y*-axis). The colour intensity of the dot represents the combined score calculated by multiplying the fold enrichment from the KEGG pathway analysis with the metabolite-gene correlation value to quantify metabolite-pathway associations. Positive correlations are in orange and negative correlations are in purple. Significant metabolites in the validation (ABOS) cohort are bolded. The clusters from the correlation analysis in Figure 2 are presented with red (cluster 1) and blue (cluster 2) bars. The larger and darker the dot, the stronger the association between the metabolite and the pathway. GPC; glycerophosphatidylcholine, GPE; glycerophosphatidylethanolamine, GPS; glycerophospatidylserine, KEGG; Kyoto Encyclopedia of Genes and Genomes, MASH; metabolic dysfunction-associated steatohepatitis, UDP-galactose; uridine diphosphate galactose.

In the KOBS cohort, pentose acid levels were lower in the livers of patients with MASH than in those with steatosis. Pentose acid was negatively associated with the histological features of MASH and fibrosis but not with steatosis. To the best of our knowledge, pentose acid has not been previously linked to MASLD or MASH. The pentose phosphate pathway is critical for the production of the reduced form of NADPH, which supports reductive biosynthesis and protects against oxidative stress [36]. Pentose acid was positively correlated with the expression of *MRPL41*, which encodes a mitochondrial ribosomal protein involved in protein synthesis within the mitochondria, suggesting a potential link between altered mitochondrial function and metabolic changes in MASH. However, pentose acid was not available in the validation cohort.

An additional novel finding of this study was that liver γ- and *β*-tocopherol and creatine levels were lower in patients with MASH than in those with steatosis. Interestingly, all three metabolites are involved in mitochondrial processes. γ- and *β*-tocopherol are products of vitamin E (α-tocopherol) metabolism. Vitamin E is an antioxidant that protects the cellular membranes from oxidative stress [37]. Vitamin E supplementation can reduce aminotransferase levels in adult patients with MASLD [38]. Interestingly, increased serum levels of α- and *β*-tocopherols have been associated with an increased probability of MASLD [39]. Creatine is an agonist for peroxisome proliferator-activated receptors α and γ (PPARα and PPARγ) [40]. PPARα is a key regulator of mitochondrial fatty acid oxidation and biogenesis, whereas PPARγ regulates adipocyte formation and insulin sensitivity [41, 42]. Creatinine and other PPAR agonists have been studied as treatment options for MASLD [43]. A similar profile of these metabolites was observed in the ABOS cohort, although the difference was not statistically significant.

We identified a novel decrease in liver guanidinosuccinate levels in patients with MASH compared to those with steatosis in the KOBS cohort. In addition, guanidinosuccinate was negatively associated with the detailed histological features of MASH, the BMI, and insulin and TG levels. Guanidino compounds are involved in nitrogen metabolism during the urea cycle, and increased levels of guanidino compounds are associated with uremia and hypertension [44]. Levels of guanidinosuccinate decrease in the rat liver after fructose exposure [45], and high dietary fructose plays a role in MASLD progression in epidemiological studies [46]. Guanidinosuccinate was associated with the expression of 82 genes, including those involved in lipid synthesis. In a linear model adjusted for age, sex, BMI and serum lipid levels, guanidinosuccinate was not significantly associated with MASH (data not shown). Guanidinosuccinate levels were not significantly different in the validation cohort. However, our results on guanidinosuccinate were linked to MASH-associated metabolic disturbances.

The 10 metabolites positively associated with MASH and belonging to cluster 1 in the correlation analysis were linked to T-cell receptor signalling and primary immunodeficiency pathways in the KEGG enrichment analysis. In contrast, 15 metabolites that were negatively associated with MASH and located in cluster 2 were linked to valine, leucine and isoleucine degradation; pyruvate metabolism; fatty acid degradation; and 2-oxocarboxylic acid metabolism pathways. Inflammatory pathways play a central role in MASH by driving immune cell activation, cytokine release and oxidative stress, which contribute to hepatocellular injury, fibrosis progression, and the transition from simple steatosis to progressive disease [47].

Our study had some limitations. The patients were severely obese (average BMI $>40\,\mathrm{kg/m^2}$), and many had type 2 diabetes; therefore, our results might not be generalisable to lean and non-obese patients with MASH [48]. Obesity may not act only as a confounder but also as a biological modifier of hepatic metabolic pathways. Although adjustment for BMI did not significantly alter the associations for most of the top metabolites, extrapolation beyond obesity-associated MASLD should be made with caution. Rapid weight loss induced by a 1 month VLCD might have affected the liver fat content [49, 50], but has a smaller effect on inflammation and fibrosis [49]. Moreover, patients in the ABOS cohort did not follow a VLCD before surgery. The study sample size limits statistical power, particularly for subgroup analyses, although we were able to detect several metabolic differences between steatosis and MASH. Importantly, we validated key findings in an external cohort. This study is cross-sectional and does not allow assessment of disease progression, regression or treatment response. Although integrations with transcriptomic and pathway analyses support biological plausibility, functional validation is required to establish mechanistic or therapeutic relevance. Finally, the utility of the metabolites as non-invasive biomarkers remains uncertain, because the majority of them were not detected in plasma samples. Future studies integrating longitudinal sampling and multi-tissue metabolomics are needed to translate these findings into clinical practice.

We performed a comprehensive non-targeted metabolomic analysis of human liver samples combined with RNA sequencing to assess the biological pathways altered between steatosis and MASH. Only a few metabolomic and lipidomic studies based on human liver samples have been performed [7, 8, 48]. We associated several novel metabolites with MASH, including N-acetylneuraminate, pentose acid, β- and γ-tocopherols, UDP-galactose and guanidinosuccinate. Finally, we validated several of the most significant metabolites in an external cohort.

Author Contributions

Conceptualisation: S.P., K.A.V., J.P. and V.M.; Resources: V.K., P.K., J.P., V.M. and D.K.; Data curation: S.P., E.F., B.S., D.E., J.T.H. and V.M.; Formal analysis: S.P. and E.F.; Methodology: S.P., J.P. and V.M.; Validation: E.F., B.S., D.E. and J.T.H., Project administration: J.P. and V.M.; Supervision: J.P. and V.M.; Visualisation: S.P.; Writing – original draft: S.P.; Writing – review and editing: S.P., E.F., K.A.V., V.K., D.K., P.K., D.E., J.T.H., V.R., R.C., F.P., B.S., J.P. and V.M.

Acknowledgements

Assistance with the study: The authors thank Editage (www.editage.com) for English language editing. Open access publishing facilitated by Ita-Suomen yliopisto, as part of the Wiley - FinELib agreement.

Funding

S.P. was supported by the Finnish Medical Foundation, Mary and Georg C. Ehrnrooth Foundation, Kuopio University Hospital Research Foundation, and State Research Funding for university-level health research. The Kuopio Obesity Surgery Study was supported by the Finnish Diabetes Research Foundation, Kuopio University Hospital Project grants (EVO/VTR grants 2005–2021), Academy of Finland grant (Contract no. 138006), Finnish Cultural Foundation, and University of Eastern Finland Spearhead Funding (J.P.). V.M. was supported by the Finnish Medical Foundation, Sigrid Jusélius Foundation, and State Research Funding for University-level health research, Kuopio University Hospital, Wellbeing Service County of North Savo. This work was also supported by the Government of France Future Investments Program (PRECINASH, ANR-16-RHUS-0006; European Genomic Institute for Diabetes, ANR-10-LABX-0046). J.T.H. received an European Research Council Starting Grant (Metabo3DC contract number: 101042759). The researchers are independent of the funders. The funding sources had no role in the design and conduct of the study; the collection, management, analysis and interpretation of the data; the preparation, review or approval of the manuscript; or the decision to submit the manuscript for publication.

Ethics Statement

The study was conducted in accordance with the principles of the Declaration of Helsinki and Istanbul. Written informed consent was obtained from all participants before the study procedure. The study protocol was approved by the Ethics Committee of Northern Savo Hospital District (54/2005, 104/2008, 27/2010 and 1108/2018).

Consent

All participants provided written informed consent.

Conflicts of Interest

The authors declare no conflicts of interest.

Data Availability Statement

The data that support the findings of this study are available from the corresponding author upon reasonable request.

References

1. K. Riazi, H. Azhari, J. H. Charette, et al., "The Prevalence and Incidence of NAFLD Worldwide: A Systematic Review and Meta-Analysis," *Lancet Gastroenterology & Hepatology* 7, no. 9 (2022): 851–861, https://doi.org/10.1016/S2468-1253(22)00165-0.

2. M. E. Rinella, J. V. Lazarus, V. Ratziu, et al., "A Multi-Society Delphi Consensus Statement on New Fatty Liver Disease Nomenclature," *Journal of Hepatology* 78 (2023): 1966–1986, https://doi.org/10.1016/j.jhep.2023.06.003.

3. E. M. Brunt, C. G. Janney, A. M. Di Bisceglie, B. A. Neuschwander-Tetri, and B. R. Bacon, "Nonalcoholic Steatohepatitis: A Proposal for Grading and Staging the Histological Lesions," *American Journal of Gastroenterology* 94, no. 9 (1999): 2467–2474, https://doi.org/10.1111/j.1572-0241.1999.01377.x.

4. M. Ekstedt, L. E. Franzén, U. L. Mathiesen, et al., "Long-Term Follow-Up of Patients With NAFLD and Elevated Liver Enzymes," *Hepatology* 44, no. 4 (2006): 865–873, https://doi.org/10.1002/hep.21327.

5. Z. M. Younossi, D. Blissett, R. Blissett, et al., "The Economic and Clinical Burden of Nonalcoholic Fatty Liver Disease in the United States and Europe," *Hepatology (Baltimore, Md.)* 64, no. 5 (2016): 1577–1586, https://doi.org/10.1002/hep.28785.

6. Z. M. Younossi, P. Golabi, J. M. Paik, A. Henry, C. Van Dongen, and L. Henry, "The Global Epidemiology of Nonalcoholic Fatty Liver Disease (NAFLD) and Nonalcoholic Steatohepatitis (NASH): A Systematic Review," *Hepatology* 77, no. 4 (2023): 1335–1347, https://doi.org/10.1097/HEP.0000000000000004.

7. M. Á. Núñez-Sánchez, M. A. Martínez-Sánchez, J. I. Martínez-Montoro, et al., "Lipidomic Analysis Reveals Alterations in Hepatic FA Profile Associated With MASLD Stage in Patients With Obesity," *Journal of Clinical Endocrinology and Metabolism* 109, no. 7 (2024): 1781–1792, https://doi.org/10.1210/clinem/dgae028.

8. P. Puri, R. A. Baillie, M. M. Wiest, et al., "A Lipidomic Analysis of Nonalcoholic Fatty Liver Disease," *Hepatology* 46, no. 4 (2007): 1081–1090, https://doi.org/10.1002/hep.21763.

9. A. D. Lake, P. Novak, P. Shipkova, et al., "Branched Chain Amino Acid Metabolism Profiles in Progressive Human Nonalcoholic Fatty Liver Disease," *Amino Acids* 47, no. 3 (2015): 603–615, https://doi.org/10.1007/s00726-014-1894-9.

10. M. Masoodi, A. Gastaldelli, T. Hyötyläinen, et al., "Metabolomics and Lipidomics in NAFLD: Biomarkers and Non-Invasive Diagnostic Tests," *Nature Reviews Gastroenterology & Hepatology* 18, no. 12 (2021): 835–856, https://doi.org/10.1038/s41575-021-00502-9.

11. E. Flam, J. T. Haas, and B. Staels, "Liver Metabolism in Human MASLD: A Review of Recent Advancements Using Human Tissue Metabolomics," *Atherosclerosis* 400 (2025): 119054, https://doi.org/10.1016/j.atherosclerosis.2024.119054.

12. J. Pihlajamaki, T. Kuulasmaa, D. Kaminska, et al., "Serum Interleukin 1 Receptor Antagonist as an Independent Marker of Non-Alcoholic Steatohepatitis in Humans," *Journal of Hepatology* 56, no. 3 (2012): 663–670, https://doi.org/10.1016/j.jhep.2011.10.005.

13. V. T. Männistö, M. Simonen, P. Soininen, et al., "Lipoprotein Subclass Metabolism in Nonalcoholic Steatohepatitis," *Journal of Lipid Research* 55, no. 12 (2014): 2676–2684, https://doi.org/10.1194/jlr.P054387.

14. V. Raverdy, F. Tavaglione, E. Chatelain, et al., "Data-Driven Cluster Analysis Identifies Distinct Types of Metabolic Dysfunction-Associated Steatotic Liver Disease," *Nature Medicine* 30, no. 12 (2024): 3624–3633, https://doi.org/10.1038/s41591-024-03283-1.

15. P. Bedossa, C. Poitou, N. Veyrie, et al., "Histopathological Algorithm and Scoring System for Evaluation of Liver Lesions in Morbidly Obese Patients," *Hepatology* 56, no. 5 (2012): 1751–1759, https://doi.org/10.1002/hep.25889.

16. D. E. Kleiner, E. M. Brunt, M. Van Natta, et al., "Design and Validation of a Histological Scoring System for Nonalcoholic Fatty Liver Disease," *Hepatology* 41, no. 6 (2005): 1313–1321, https://doi.org/10.1002/hep.20701.

17. V. Männistö, D. Kaminska, P. Käkelä, et al., "Protein Phosphatase 1 Regulatory Subunit 3B Genotype at rs4240624 Has a Major Effect on Gallbladder Bile Composition," *Hepatology Communications* 5, no. 2 (2021): 244–257, https://doi.org/10.1002/hep4.1630.

18. J. Thaiparambil, J. Dong, S. L. Grimm, et al., "Integrative Metabolomics and Transcriptomics Analysis Reveals Novel Therapeutic Vulnerabilities in Lung Cancer," *Cancer Medicine* 12, no. 1 (2023): 584–596, https://doi.org/10.1002/cam4.4933.

19. L. Deng, W. Li, W. Liu, et al., "Integrative Metabolomic and Transcriptomic Analysis Reveals Difference in Glucose and Lipid Metabolism in the Longissimus Muscle of Luchuan and Duroc Pigs," *Frontiers in Genetics* 14 (2023): 1128033, https://doi.org/10.3389/fgene.2023.1128033.

20. S. K. Bansal and M. B. Bansal, "Pathogenesis of MASLD and MASH – Role of Insulin Resistance and Lipotoxicity," *Alimentary Pharmacology & Therapeutics* 59, no. 1 (2024): S10–S22, https://doi.org/10.1111/apt.17930.

21. M. Rajappa, S. Ikkruthi, H. Nandeesha, et al., "Relationship of Raised Serum Total and Protein Bound Sialic Acid Levels With Hyperinsulinemia and Indices of Insulin Sensitivity and Insulin Resistance in Non-Diabetic Normotensive Obese Subjects," *Diabetes & Metabolic Syndrome* 7, no. 1 (2013): 17–19, https://doi.org/10.1016/j.dsx.2013.02.030.

22. Z. Lu, H. Ma, C. Xu, Z. Shao, C. Cen, and Y. Li, "Serum Sialic Acid Level Is Significantly Associated With Nonalcoholic Fatty Liver Disease in a Nonobese Chinese Population: A Cross-Sectional Study," *BioMed Research International* 2016 (2016): 5921589, https://doi.org/10.1155/2016/5921589.

23. M. A. Crook, J. C. Pickup, P. J. Lumb, et al., "Relationship Between Plasma Sialic Acid Concentration and Microvascular and Macrovascular Complications in Type 1 Diabetes: The EURODIAB Complications Study," *Diabetes Care* 24, no. 2 (2001): 316–322, https://doi.org/10.2337/diacare.24.2.316.

24. R. Iijima, T. Ichikawa, and M. Yamazaki, "Sialic Acid Attenuates the Cytotoxicity of the Lipid Hydroperoxides HpODE and HpETE," *Carbohydrate Research* 344, no. 7 (2009): 933–935, https://doi.org/10.1016/j.carres.2009.02.025.

25. M. M. Adeva-Andany, N. Pérez-Felpete, C. Fernández-Fernández, C. Donapetry-García, and C. Pazos-García, "Liver Glucose Metabolism in Humans," *Bioscience Reports* 36, no. 6 (2016): e00416, https://doi.org/10.1042/BSR20160385.

26. E. Bieberich, "Synthesis, Processing, and Function of N-Glycans in N-Glycoproteins," *Advances in Neurobiology* 29 (2023): 65–93, https://doi.org/10.1007/978-3-031-12390-0_3.

27. X. Verhelst, A. M. Dias, J. F. Colombel, et al., "Protein Glycosylation as a Diagnostic and Prognostic Marker of Chronic Inflammatory Gastrointestinal and Liver Diseases," *Gastroenterology* 158, no. 1 (2020): 95–110, https://doi.org/10.1053/j.gastro.2019.08.060.

28. B. Blomme, S. Francque, E. Trépo, et al., "N-Glycan Based Biomarker Distinguishing Non-Alcoholic Steatohepatitis From Steatosis Independently of Fibrosis," *Digestive and Liver Disease* 44, no. 4 (2012): 315–322, https://doi.org/10.1016/j.dld.2011.10.015.

29. Y. Yamasaki, K. Nouso, K. Miyahara, et al., "Use of Non-Invasive Serum Glycan Markers to Distinguish Non-Alcoholic Steatohepatitis From Simple Steatosis," *Journal of Gastroenterology and Hepatology* 30, no. 3 (2015): 528–534, https://doi.org/10.1111/jgh.12726.

30. I. Mederacke, A. Filliol, S. Affo, et al., "The Purinergic P2Y14 Receptor Links Hepatocyte Death to Hepatic Stellate Cell Activation and Fibrogenesis in the Liver," *Science Translational Medicine* 14, no. 639 (2022): eabe5795, https://doi.org/10.1126/scitranslmed.abe5795.

31. D. Geh, D. M. Manas, and H. L. Reeves, "Hepatocellular Carcinoma in Non-Alcoholic Fatty Liver Disease—A Review of an Emerging Challenge Facing Clinicians," *Hepatobiliary Surgery and Nutrition* 10, no. 1 (2021): 59–75, https://doi.org/10.21037/hbsn.2019.08.08.

32. R. Maeba and N. Ueta, "Ethanolamine Plasmalogens Prevent the Oxidation of Cholesterol by Reducing the Oxidizability of Cholesterol in Phospholipid Bilayers," *Journal of Lipid Research* 44, no. 1 (2003): 164–171, https://doi.org/10.1194/jlr.M200340-JLR200.

33. M. Zommara, N. Tachibana, K. Mitsui, et al., "Inhibitory Effect of Ethanolamine Plasmalogen on Iron- and Copper-Dependent Lipid Peroxidation," *Free Radical Biology & Medicine* 18, no. 3 (1995): 599–602, https://doi.org/10.1016/0891-5849(94)00155-D.

34. A. Ikuta, T. Sakurai, M. Nishimukai, et al., "Composition of Plasmalogens in Serum Lipoproteins From Patients With Non-Alcoholic Steatohepatitis and Their Susceptibility to Oxidation," *Clinica Chimica Acta* 493 (2019): 1–7, https://doi.org/10.1016/j.cca.2019.02.020.

35. T. Paavola, U. Bergmann, S. Kuusisto, S. Kakko, M. J. Savolainen, and T. Salonurmi, "Distinct Fatty Acid Compositions of HDL Phospholipids Are Characteristic of Metabolic Syndrome and Premature Coronary Heart Disease—Family Study," *International Journal of Molecular Sciences* 22, no. 9 (2021): 4908, https://doi.org/10.3390/ijms22094908.

36. E. S. Jin, M. H. Lee, R. E. Murphy, and C. R. Malloy, "Pentose Phosphate Pathway Activity Parallels Lipogenesis but Not Antioxidant Processes in Rat Liver," *American Journal of Physiology. Endocrinology and Metabolism* 314, no. 6 (2018): E543–E551, https://doi.org/10.1152/ajpendo.00342.2017.

37. K. Jomova, R. Raptova, S. Y. Alomar, et al., "Reactive Oxygen Species, Toxicity, Oxidative Stress, and Antioxidants: Chronic Diseases and Aging," *Archives of Toxicology* 97, no. 10 (2023): 2499–2574, https://doi.org/10.1007/s00204-023-03562-9.

38. S. Vogli, A. Naska, G. Marinos, M. I. Kasdagli, and P. Orfanos, "The Effect of Vitamin E Supplementation on Serum Aminotransferases in Non-Alcoholic Fatty Liver Disease (NAFLD): A Systematic Review and Meta-Analysis," *Nutrients* 15, no. 17 (2023): 3733, https://doi.org/10.3390/nu15173733.

39. W. Chai and M. H. Tao, "Overall and Sex-Specific Associations of Serum Lipid-Soluble Micronutrients With Metabolic Dysfunction-Associated Steatotic Liver Disease Among Adults in the United States," *Nutrients* 16, no. 8 (2024): 1242, https://doi.org/10.3390/nu16081242.

40. R. Deminice, G. S. de Castro, M. E. Brosnan, and J. T. Brosnan, "Creatine Supplementation as a Possible New Therapeutic Approach for Fatty Liver Disease: Early Findings," *Amino Acids* 48, no. 8 (2016): e21836, https://doi.org/10.1007/s00726-016-2183-6.

41. M. Pawlak, P. Lefebvre, and B. Staels, "Molecular Mechanism of PPARα Action and Its Impact on Lipid Metabolism, Inflammation and Fibrosis in Non-Alcoholic Fatty Liver Disease," *Journal of Hepatology* 62, no. 3 (2015): 720–733, https://doi.org/10.1016/j.jhep.2014.10.039.

42. M. Ahmadian, J. M. Suh, N. Hah, et al., "PPARγ Signaling and Metabolism: The Good, the Bad and the Future," *Nature Medicine* 19, no. 5 (2013): 3159, https://doi.org/10.1038/nm.3159.

43. N. S. Choudhary, N. Kumar, and A. Duseja, "Peroxisome Proliferator-Activated Receptors and Their Agonists in Nonalcoholic Fatty Liver Disease," *Journal of Clinical and Experimental Hepatology* 9, no. 6 (2019): 731–739, https://doi.org/10.1016/j.jceh.2019.06.004.

44. M. Chmielewski, O. Heimbürger, P. Stenvinkel, and B. Lindholm, "Chapter 4 - Uremic Toxicity," in *Nutritional Management of Renal Disease*, ed. J. D. Kopple, S. G. Massry, and K. Kalantar-Zadeh (Academic Press, 2013), 49–77, https://doi.org/10.1016/B978-0-12-391934-2.00004-7.

45. O. Rang, X. Qin, Y. Tang, et al., "The Effect of Fructose Exposure on Amino Acid Metabolism Among Chinese Community Residents and Its Possible Multi-Omics Mechanisms," *Scientific Reports* 13, no. 1 (2023): 22704, https://doi.org/10.1038/s41598-023-50069-5.

46. K. Burger, M. Michael Trauner, and I. Bergheim, “Pathogenic Aspects of Fructose Consumption in Metabolic Dysfunction-Associated Steatotic Liver Disease (MASLD): A Narrative Review,” *Cell Stress* 9 (2025): 49–64, https://doi.org/10.15698/cst2025.06.305.

47. L. Rabiu, P. Zhang, L. O. Afolabi, et al., “Immunological Dynamics in MASH: From Landscape Analysis to Therapeutic Intervention,” *Journal of Gastroenterology* 59, no. 12 (2024): 1053–1078, https://doi.org/10.1007/s00535-024-02157-0.

48. A. Sourianarayanane, C. R. Brydges, and A. J. McCullough, “Liver Tissue Lipids in Metabolic Dysfunction-Associated Steatotic Liver Disease With Diabetes and Obesity,” *Clinical Research in Hepatology and Gastroenterology* 48, no. 7 (2024): 102402, https://doi.org/10.1016/j.clinre.2024.102402.

49. M. C. Lewis, M. L. Phillips, J. P. Slavotinek, L. Kow, C. H. Thompson, and J. Toouli, “Change in Liver Size and Fat Content After Treatment With Optifast Very Low Calorie Diet,” *Obesity Surgery* 16, no. 6 (2006): 697–701, https://doi.org/10.1381/096089206777346682.

50. A. Khemtong, P. C. Shantavasinkul, P. Boonchaya-Anant, S. Rattanasiri, S. Treeprasertsuk, and S. Udomsawaengsup, “Effect of Preoperative Very Low-Calorie Diets on Hepatic Steatosis, Fibrosis, and Perioperative Outcomes of Bariatric Surgery,” *Journal of Laparoendoscopic & Advanced Surgical Techniques. Part A* 34, no. 3 (2024): 219–226, https://doi.org/10.1089/lap.2023.0391.

Supporting Information

Additional supporting information can be found online in the Supporting Information section. **Figure S1:** Results of the primary component analysis between patients with steatosis and MASH. MASH; metabolic dysfunction-associated steatotic liver disease, PCA; primary component analysis. **Figure S2:** A forest plot representing all metabolites that differed significantly between patients with steatosis and MASH in a linear model adjusted with age and sex. The lines around the dots represent 95% confidence interval. Raw *p*-value (*p*) <0.05 was considered significant. GPC; glycerophosphatidylcholine, GPE; glycerophosphatidylethanolamine, GPS; glycerophospatidylserine, MASH; metabolic dysfunction-associated steatohepatitis, Psig; raw *p*-value, UDP-galactose; uridine diphosphate galactose. **Figure S3:** A forest plot representing how top 25 metabolites that differed significantly between patients with steatosis and MASH in a linear model adjusted with age and sex behaved in a linear model adjusted with age, sex, and BMI. The metabolites that were significant in both KOBS and ABOS cohorts in a model adjusted with age and sex are bolded. The lines around the dots represent 95% confidence interval. Raw *p*-value (*p*) <0.05 was considered significant, represented in red in the figure. BMI; body mass index, GPC; glycerophosphatidylcholine, GPE; glycerophosphatidylethanolamine, GPS; glycerophospatidylserine, MASH; metabolic dysfunction-associated steatohepatitis, Psig; raw *p*-value, UDP-galactose; uridine diphosphate galactose. **Figure S4:** A forest plot representing how top 25 metabolites that differed significantly between patients with steatosis and MASH in a linear model adjusted with age and sex behaved in a linear model adjusted with age, sex, and PNPLA3, TM6SF2 and MBOAT7 risk variants. The metabolites that were significant in both KOBS and ABOS cohorts in a model adjusted with age and sex are bolded. The lines around the dots represent 95% confidence interval. Raw *p*-value (*p*) <0.05 was considered significant, represented in red and blue in the figure. GPC; glycerophosphatidylcholine, GPE; glycerophosphatidylethanolamine, GPS; glycerophospatidylserine, MASH; metabolic dysfunction-associated steatohepatitis, MBOAT7; membrane-bound O-acyltransferase domain containing 7, PNPLA3; Patatin-like phospholipase domain containing 3, Psig; raw *p*-value, TM6SF2; transmembrane 6 superfamily member, UDP-galactose; uridine diphosphate galactose. **Figure S5:** A forest plot representing how top 25 metabolites that differed significantly between patients with steatosis and MASH in a linear model adjusted with age and sex behaved in a linear model adjusted with age, sex, and usage of cholesterol medication. The metabolites that were significant in both KOBS and ABOS cohorts in a model adjusted with age and sex are bolded. The lines around the dots represent 95% confidence interval. Raw *p*-value (*p*) <0.05 was considered significant, represented in red and blue in the figure. GPC; glycerophosphatidylcholine, GPE; glycerophosphatidylethanolamine, GPS; glycerophospatidylserine, MASH; metabolic dysfunction-associated steatohepatitis, Psig; raw *p*-value. **Figure S6:** A forest plot representing how top 25 metabolites that differed significantly between patients with steatosis and MASH in a linear model adjusted with age and sex behaved in a linear model adjusted with age, sex and type 2 diabetes status. The metabolites that were significant in both KOBS and ABOS cohorts in a model adjusted with age and sex are bolded. The lines around the dots represent 95% confidence interval. Raw *p*-value (*p*) <0.05 was considered significant, represented in red and blue in the figure. GPC; glycerophosphatidylcholine, GPE; glycerophosphatidylethanolamine, GPS; glycerophospatidylserine, MASH; metabolic dysfunction-associated steatohepatitis, Psig; raw *p*-value. **Figure S7:** Heatmap representing associations (Spearman's correlation adjusted with age and sex) between metabolites differing significantly between patients with steatosis and MASH (on vertical row) and insulin, glucose, cholesterol, LDL cholesterol, HDL cholesterol and TGs, BMI (horizontal row, left side of the panel), and liver histology (horizontal row, right side of the panel). *K*-means clustering is used for clustering the metabolites based on their metabolic and histologic associations. * represents statistically significant correlation ($p<0.05$). Positive correlation is presented as shades of orange and negative correlations with shades of purple. GPC; glycerophosphatidylcholine, GPE; glycerophosphatidylethanolamine, GPS; glycerophospatidylserine, HDL-Chol; high-density lipoprotein cholesterol, LDL-Chol; low-density lipoprotein cholesterol, MASH; metabolic dysfunction-associated steatohepatitis, TG; triglyceride, UDP-galactose; uridine diphosphate galactose. **Table S1:** Clinical characteristics of the ABOS (validation) cohort. **Table S2:** Results of Student's *t*-tests conducted to assess how the metabolites differed among all histological groups (normal liver, steatosis and MASH). **Table S3:** Results of a linear model run between patients with steatosis and patients with MASH, adjusted with age and sex. **Table S4:** Results of a linear model between patients with steatosis and patients with MASH, adjusted with age, sex, and BMI, in the KOBS cohort. **Table S5:** Results of a linear model between patients with steatosis and patients with MASH, adjusted with age and sex, in the ABOS cohort. **Table S6:** Results of a linear model between patients with steatosis and patients with MASH, adjusted with age and sex, plasma metabolomics, in the ABOS cohort. **Table S7:** Results (all gene-expression-metabolite correlations with FDR <0.1) from a partial Spearman correlation analysis, controlled for age, sex and BMI, in the KOBS cohort, $n=34$.